Nature Environment and Pollution Technology
An International Quarterly Scientific Journal

p-ISSN: 0972-6268
(Print copies up to 2016)
e-ISSN: 2395-3454

Vol. 24 | No. 1 | Article ID D1688 | 2025

Original Research Paper

https://doi.org/10.46488/NEPT.2025.v24i01.D1688

Open Access Journal

The Synthesis of AgNPs/SAC Using Banana Frond Extract as a Bioreducing Agent and its Application as Photocatalyst in Methylene Blue Degradation

Anti Kolonial Prodjosantoso†, Tengku Khadijah Nurul Hanifah, Maximus Pranjoto Utomo, Cornelia Budimarwanti and Lis Permana Sari

Department of Chemistry, Yogyakarta State University, Yogyakarta, Indonesia

†Corresponding author: Anti Kolonial Prodjosantoso; prodjosantoso@uny.ac.id

Abbreviation: Nat. Env. & Poll. Technol.
Website: www.neptjournal.com

Received: 10-06-2024
Revised: 15-07-2024
Accepted: 17-07-2024

Key Words:

AgNPs/SAC
Bioreducing agent
Photodegradation effectiveness
Methylene blue
Banana frond extract

Citation for the Paper:

Prodjosantoso, A.K., Hanifah, T.K.N., Utomo, M.P., Budimarwanti, C. and Sari, L.P., 2025. The synthesis of AgNPs/SAC using banana frond extract as a bioreducing agent and its application as photocatalyst in methylene blue degradation. *Nature Environment and Pollution Technology*, 24(1), D1688. https://doi.org/10.46488/NEPT.2025.v24i01.D1688

Note: From year 2025, the journal uses Article ID instead of page numbers in citation of the published articles.

ABSTRACT

Silver nanoparticles (AgNPs) were synthesized utilizing various methods, including bioreducing agents. The synthesis involved the use of silver nitrate ($AgNO_3$) as the precursor and banana frond extract as the bioreducing agent, with different volume ratios being tested. Subsequently, the most optimal variant of AgNPs was immobilized onto activated carbon (AC) derived from soybean seeds. The AgNPs/SAC composite was subjected to thorough characterization using UV-Vis diffuse reflectance spectroscopy and X-ray diffraction (XRD). A series of degradation experiments were then conducted using methylene blue, with the reaction duration following a specific protocol. A comparison of methylene blue concentrations before and after the photodegradation process was made to assess the reaction's efficacy. The findings revealed that the ideal ratio between the bioreducing agent and precursor was 9:30 (v/v). The AgNPs/SAC composite exhibited a peak absorption at a wavelength of 420-440 nm. The UV-DRS characterization of AgNPs/SAC unveiled a band gap energy of 1.52 eV. The AgNPs supported on AC displayed a peak absorption wavelength of 5,438.5 nm, showcasing a face-centered cubic (FCC) structure. The AgNPs/SAC effectively decreased the concentration of methylene blue through a combination of adsorption and photodegradation mechanisms, achieving efficiencies of 35.3813% and 81.1636%, respectively. The AgNPs/SAC composite demonstrates significant potential for efficient and sustainable water treatment.

INTRODUCTION

The textile industry generates 10-15% of the total dyestuff waste during dyeing (Jyoti & Singh 2016). Dyes are organic compounds with aromatic structures, known for their high stability and difficulty to degrade (Daneshvar et al. 2007). One of the most commonly used dyes is methylene blue. The issue of dye waste can be mitigated through various methods, including biosensing, adsorption, filtration, electrolysis, coagulation, and sedimentation (Ong 2011, Thenarasu et al. 2024). These methods, when implemented, often do not yield optimal results, are difficult to execute, and can sometimes even create new problems. The method of waste treatment using photocatalysts was developed due to its advantages.

Nanoparticles have a high surface-to-volume ratio, enhancing their reactivity and allowing for the development of more efficient and effective water treatment technologies (Cao et al. 2024). Among the nanoparticles that can be employed as photocatalysts are silver nanoparticles (AgNPs). Silver metal (Ag) exhibits excellent photocatalytic properties (Wahyuni et al. 2017). A variety of techniques have been developed for synthesizing AgNPs, including chemical reduction methods (Kumar et al. 2015), electrochemical reduction, bioreduction (Mubarak et al. 2011, Silambarasan & Jayanthi 2013), sol-gel (Lenzi et al. 2011), and photoreduction (Chan & Barteau

2005). The bioreduction method is known as environmentally friendly (Jyoti & Singh 2016, Ma et al. 2024).

Plant extracts contain a variety of secondary metabolites, including alkaloids, tannins, flavonoids, steroids, and phenols. These compounds can act as reducing and stabilizing agents of silver nanoparticles. One example of a plant that contains secondary metabolites is the banana frond. The ethanolic extract of banana frond contains flavonoids, tannins, and saponins (Fatma 2018).

Nanoparticles supported within larger materials are employed to enable the repeated use of nanoparticles, which are firmly anchored to the supporting material. Activated carbon stands out as a suitable support material due to its beneficial characteristics, such as large surface area, resilience to acidic and alkaline conditions, and the ability to modify its functional groups. The functional groups on the surface of carbon can function as a support for the developed metal catalyst or become active sites for specific catalytic reactions (Gläsel 2015). Soybeans are one of the natural sources from which activated carbon can be derived.

Based on the preceding description, this study focuses on the synthesis of AgNPs/SAC using the banana frond extract (*Musa balbisiana*) as a bioreducing agent and its application as a photocatalyst for methylene blue degradation. The resulting AgNPs/SAC were characterized using UV-Vis DRS and XRD, and then their photocatalytic effectiveness against methylene blue was evaluated.

MATERIALS AND METHODS

The main materials used in the experiment include $AgNO_3$ (Sigma Aldrich 99.9999%), methylene blue (Sigma Aldrich >995%), and banana frond extract (*Musa balbisiana*); and the instruments were UV-Vis Spectrophotometer (Shimadzu 2400 PC Series), UV-Vis DRS (Shimadzu UV-2450 spectrophotometer), XRD (Rigaku miniflex 600, and photochemical reactor (Techinstro).

The banana frond extract was obtained by using an extraction procedure implemented following the methodology proposed by Prodjosantoso et al. (2019). The frond of the banana was cut into small pieces, washed, and dried at room temperature. A total of 25 grams of dried banana frond were combined with 150 milliliters of distilled water and blended for five minutes using a blender. Subsequently, filtration was conducted using filter paper (Whatman Grade 42).

The activated carbon (AC) preparation method was carried out by modifying the Hatina method (Rampe & Tiwow 2018). Soybean seeds were first washed with distilled water and then sun-dried for four hours. They were subsequently oven-dried at a temperature of 105°C for 24 hours. A total of dry 250 grams of soybean seeds were then subjected to a heating process at a temperature of 500°C for four hours. Following this, the seeds were washed and activated using a solution of hydrochloric acid (HCl 0.1 M) in a ratio of 1:2 (w/v) for ten hours. The seeds were then rinsed with distilled water and activated using sodium hydroxide (NaOH 0.1 M) in a ratio of 1:2 (w/v) for ten hours. Finally, the seeds were rinsed again with distilled water and dried in an oven at a temperature of 105 °C for two hours.

A total of 30 mL of $AgNO_3$ 0.01 M solution was prepared in six separate Erlenmeyer flasks. Subsequently, add 3, 4.5, 6, 7.5, 9, and 10.5 mL of banana frond extract to respective flasks. The mixture is then stirred with a magnetic stirrer for two hours. After stirring, the solutions were analyzed using a UV-Vis spectrophotometer to determine the optimal variation.

The synthesis of AgNPs in this study followed the method developed by Taba et al. (2022). First, 100 mL of 0.01 M $AgNO_3$ was introduced into the beaker, and a specific quantity of banana frond extract was added according to the optimal composition. The mixture was then stirred for two hours using a magnetic stirrer. The impregnation of AgNPs onto SAC was adapted from the Nguyen et al. (2020) method. Subsequently, 25 g of activated carbon was added to the mixture, which was then tightly covered using aluminum foil. The mixture was then shaken for 24 hours. The AgNPs/SAC were then filtered, washed with ethanol, and dried in an oven at 110°C oven for 2 hours. The resulting AgNPs/SAC were characterized using UV-Vis DRS and XRD methods.

A 100 ppm stock solution was prepared by dissolving 100 mg of methylene blue in 1 L of distilled water. This stock solution was then diluted to prepare standard solutions with concentrations of 1, 2, 4, 6, and 8 ppm. The absorbance of these standard solutions was measured using a UV-Vis spectrophotometer.

Photodegradation was studied by using the method published by Prodjosantoso (2019), which was by adding 1 g of AgNPs/SAC into 100 mL of a 50 ppm methylene blue solution. The mixture was placed in an Erlenmeyer flask and agitated at various time intervals (0, 5, 10, 15, 30, 60, 120, and 180 minutes) in the dark. After 24 hours, the mixture was exposed to the sunlight for photodegradation within time intervals of 0, 5, 10, 15, 30, 60, 120, and 180 minutes. The final concentration of methylene blue was then measured using a UV-Vis spectrophotometer to calculate the photodegradation effectiveness.

RESULTS AND DISCUSSION

The optimal bioreducing agent and the precursor volume ratio were of interest in the formation of AgNPs. The optimal

composition is determined by the highest absorbance of the typical wavelengths of the analyzed particles. Qualitatively, a higher absorbance indicates a greater number of AgNPs formed, implying a higher concentration of AgNPs in the solution. The shifting of the wavelength position to the larger wavelength indicates the lower stability of the AgNPs (De Leersnyder et al. 2019).

A combination treatment of agitating and stirring of the mixtures of $AgNO_3$ 0.01 M solution and bioreducing agents resulted in the formation of silver nanoparticles characterized by the solution color change from yellow to brownish. This color change is assumed due to the reduction of Ag^+ ions to Ag^0 by secondary metabolites in the banana frond extract. This phenomenon, known as surface plasmon resonance (SPR), can be observed using a UV-Vis spectrophotometer in the range of 400-500 nm (Melkamu & Bitew 2021). The coloration observed in the solution of AgNPs is illustrated in Fig. 1.a.

Fig. 1.b. Indicates that the most stable AgNPs are achieved with a 9 mL variation of bioreducing agent. Additionally, the differences in wavelength can indicate variations in the particle size of AgNPs, with smaller particles being characterized by shorter wavelengths (Asif et al. 2022). From the absorbance perspective, the 9 mL variation exhibits the highest absorbance value of 0.242. The high absorbance is directly proportional to the number of AgNPs formed. Consequently, the 9:30 (v/v) variation was selected as the optimal composition, as it exhibited the most intense brown color, the highest absorbance, and the shortest wavelength.

The bandgap energy disparity also influences the energy of photons or the quantity of light required. The reduction in bandgap energy necessitates a proportional decrease in light energy, and vice-versa (Dhankhar et al. 2014). Consequently, the bandgap energy is determined to ascertain the photocatalytic activity of a photocatalyst. In this study, the bandgap energy was determined using a DRS spectrophotometer instrument in the ultraviolet-visible light area. To obtain the bandgap energy, the data is processed using the Kubelka-Munk equation, as follows:

Where F (R) is the Kubelka-Munk factor, R is the reflectance, A is the proportional constant, and Eg is the gap energy (eV) (Landi et al. 2022). The results of these

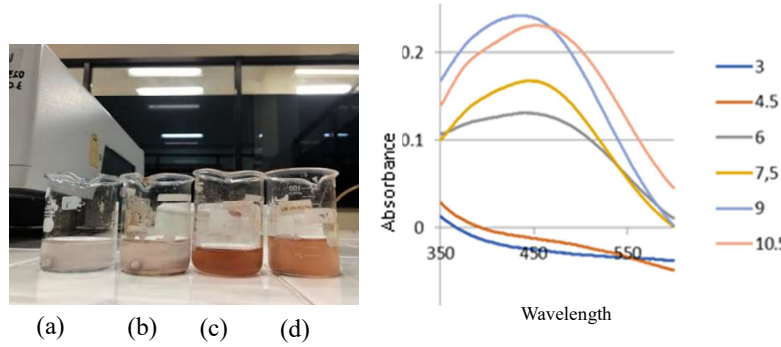

Fig. 1: (a) AgNPs color solutions obtained by adding a) 6 mL, b) 7.5 mL, c) 9 mL, and d) 10.5 mL bioreducing agent; and (b) Bioreducing agent composition optimization curve.

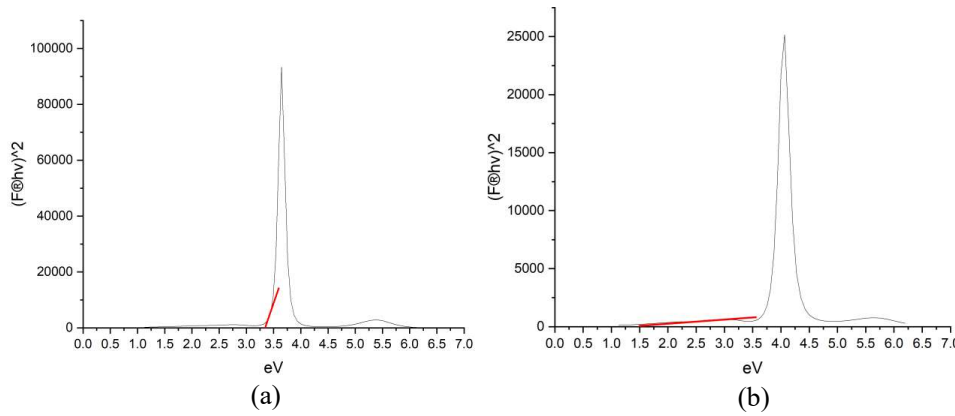

Fig. 2: Bandgap Energy Curves of a) AC and b) AgNPs/SAC.

calculations are then processed into curves. The linear portion of the curve is extrapolated in a direction perpendicular to the X-axis to obtain the bandgap energy value. The bandgap energy curve is presented in Fig. 2.

Fig. 2 indicates that the bandgap energies of AC and AgNPs/SAC are 3.33 eV and 1.52 eV, respectively. These findings demonstrate that the incorporation of AgNPs into SAC results in a significant reduction in the bandgap energy. This reduction can be attributed to the formation of new electronic levels. A lower bandgap energy indicates that electrons are more readily excited from the valence band to the conduction band when exposed to photon energy. According to Rizki et al., the bandgap energy reduction of composites can facilitate the formation of electron-hole (e^- - h^+) pairs during light irradiation, thereby enhancing photocatalytic activity (Rizki et al. 2023).

The X-ray diffraction (XRD) method is a widely utilized analytical technique for analyzing crystal structures and particle sizes (Kumar & Hymavathi 2017). Each crystal exhibits a unique diffraction pattern. In this study, XRD characterization was conducted using Cu-Kα radiation sources at 2θ angles between 10-90º to determine the crystal size of AgNPs supported by AC. The diffractograms of AC and AgNPs/SAC were compared to identify the specific peaks of AgNPs. These peaks were then compared to data from COD (Crystallography Open Database). The XRD analysis results indicate that AC is an amorphous material. The diffractogram pattern of AC is presented in Fig. 3.

Fig. 3.a illustrates the presence of multiple peaks, two observed at 2θ angles of approximately 26° and 46°. This is consistent with the findings of Jain et al. (2021), which indicate that the amorphous peak of AC occurs at 2θ around 26° and 43°. The peak at 2θ about 25° corresponds to the diffraction (002) derived from graphite (Ahmad et al. 2003). The diffraction pattern of AgNPs/SAC differs slightly from that of AC. The appearance of sharp peaks in the AgNP/AC diffractogram indicates that AgNPs have been successfully loaded onto the AC (Tuan et al. 2011). Wide peaks indicate small particle sizes (Sudhakar & Soni 2018).

Some peaks have emerged at 2θ values of 38.40°; 44.45°; 64.65°; 77.43°; and 81.83°, which respectively represent the hkl planes (111), (002), (022), (113), and (222) (Fig. 3.b). The (111) plane was the most intense, indicating that the AgNPs orientation was along this plane. This finding is consistent with the results of the research conducted by Isa and Lockman (2019). The analysis results indicated the formation of AgNPs with a face-centered cubic (FCC) structure, which aligns with previous research by Isa & Lockman (2019).

X-ray diffraction (XRD) data are also employed to determine the crystal size of AgNPs. The determination of the crystal size is calculated using the Debye-Scherrer equation:

$$D = \frac{k\lambda}{\beta \cos\theta}$$

Where D represents the crystal size in nanometers, k is a dimensionless shape factor (typically 0.89), λ is the wavelength (nm), β is the FWHM (full width at half maximum) value, and θ is the Bragg angle (deg) (Radha & Thamilselvi 2013). The calculations indicate that AgNPs supported by AC have an average size of 5.4385 nm. These results are similar to those found in Nisa's (2024) research where she synthesized AgNPs/SAC using banana pith extract, obtaining a particle size of 13.69±5.11 nm.

The methylene blue adsorption on the AgNPs/SAC was studied in the dark to prevent photocatalysis. This dark state is achieved by covering the surface of the Erlenmeyer flask

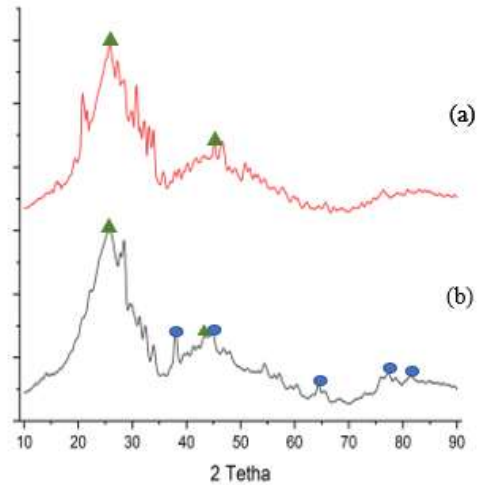

Fig. 3: XRD pattern of a) AC and b) AgNPs/SAC.

Table 1: Methylene blue in the solutions.

Time (minutes)	0	5	10	15	30	60	120	180
Concentration (ppm)	50.81752	48.79924	47.27605	45.84606	42.30494	39.68738	38.05468	32.83763

Table 2: Methylene blue in the solution after the photodegradation processes.

Time (minutes)	0	5	10	15	30	60	120	180
Concentration (ppm)	31.73829	29.88906	28.28117	26.50954	21.82125	15.597	8.73449	5.97836

with aluminum foil. The shaking process is carried out at specific time intervals. The data on the concentrations of methylene blue at various time intervals can be found in Table 1.

The data (Table 1.) indicate that the concentration of methylene blue decreases along with increasing light exposure time. The relationship between reaction rate and concentration can be determined using the reaction order equation, as follows:

1) Zero Reaction Order

$$C_t = -kt + C_0$$

2) First Reaction Order

$$lnC_t = -kt + ln\, C_0$$

3) Second Reaction Order

$$1/C_t = -kt + 1/C_0$$

The concentration of methylene blue at time t (ppm), k is the rate constant; t is the time (minutes); and C_0 is the initial concentration of methylene blue (ppm) (Sun 2014). The reaction order is determined by comparing the R^2 values for each reaction order curve. The reaction order with the greatest R^2 value indicates the order of the reaction. The R^2 values for the zero-order, first-order, and second-order reactions were 0.8873, 0.9175, and 0.9829, respectively. These results indicate that the adsorption reaction follows the second-order kinetics.

The adsorption effectiveness of methylene blue is calculated using the following equation:

$$\%\text{Efficacy} = \frac{C_0 - C_e}{C_o} \times 100\%$$

The calculations indicate that the effectiveness of AC adsorption is 35.3813%.

Following 24 hours of adsorption in the absence of light, photodegradation of methylene blue is initiated. This study assumes that after a 24-hour adsorption period, no further adsorption occurs and that the subsequent reaction is solely a photodegradation reaction of AgNPs. It should be noted, however, that this study does not guarantee that the photodegradation process occurs without a simultaneous adsorption process.

The photodegradation process is conducted under sunlight, with time intervals of 0, 5, 10, 15, 30, 60, 120, and 180 minutes. The utilization of sunlight as a light source is predicated on the energy value of the band gap of AgNPs, wherein AgNPs exhibit photocatalytic activity in the visible light spectrum. Sunlight is comprised of 38.9% visible light, 6.8% ultraviolet light, and 54.3% infrared light. Furthermore, the use of solar energy, particularly sunlight, is energy-saving, given that the sun is a renewable energy source. The photodegradation process was conducted between 10:00 a.m. and 1:00 p.m., with the measured light intensity on the lux meter ranging from 4,000 to 8,000 lux. When the catalyst in solution is irradiated by light, electron-hole pairs are formed on the catalyst surface. The excitation of electrons from the valence band to the conduction band is accompanied by the formation of a positive hole, resulting in the production of an electron-hole pair. Both charge carriers will undergo redox reactions to produce hydroxyl radicals (OH*) and superoxide radicals (O*). Hydroxyl radicals possess strong oxidizing properties and exhibit a considerable redox potential, enabling them to oxidize most organic substances into water, hydroxyl acids, and carbon dioxide (Wat et al. 2011). Consequently, the concentration of organic substances, such as methylene blue, is reduced. The results of the photodegradation process, as evidenced by a decrease in the concentration of methylene blue, are presented in Table 2.

The rate of photodegradation can be determined based on the equation of the line on the second-order curve, using the following equation:

$$r = k\, C^n$$

Where r is the reaction rate (ppm/min), C is the concentration (ppm), k is the reaction rate constant, and n is the reaction order (Chiu 2019). The photodegradation reaction rate of methylene blue using AgNPs was calculated to be 0.8058 ppm/minute. The efficacy of the photodegradation process was evaluated by comparing the decline in the concentration of methylene blue to its initial concentration. The results demonstrated a reduction in the concentration of methylene blue from 31.73829 ppm to 5.97836 ppm,

indicating an 81.1636% effectiveness of methylene blue photodegradation by AgNPs/SAC. Consequently, the effectiveness of photodegradation is greater than that of adsorption.

CONCLUSIONS

The research findings reveal that the optimal proportion of banana frond extract combined with precursors is 9:30 (v/v), demonstrating the highest absorbance value at the 437 nm wavelength. The bandgap energy of AgNPs/SAC is 1.52 eV, with AgNPs particles supported on AC exhibiting an FCC structure and an average particle size of 5.4385 nm. The adsorption efficiency of AgNPs/SAC stands at 35.3813%, while the photodegradation effectiveness reaches 81.1636%. The application of AgNPs/SAC proves to be highly effective in water treatment.

ACKNOWLEDGMENTS

We express our gratitude to Yogyakarta State University for the funding of the research project entitled “The Synthesis of AgNPs/SAC using banana frond extract as a bioreducing agent and its utilization as a photocatalyst in the degradation of methylene blue”.

REFERENCES

Ahmad, A., Senapati, S., Khan, M.I., Kumar, R. and Sastry, M., 2003. Extracellular biosynthesis of monodisperse gold nanoparticles by a novel extremophilic actinomycete, *Thermomonospora* sp. *Langmuir*, 19(8), pp.3550-3553.

Amri, F.S. and Hossain, M.A., 2018. Comparison of total phenols, flavonoids and antioxidant potential of local and imported ripe bananas. *Egyptian Journal of Basic and Applied Sciences*, 5(4), pp.245-251.

Asif, M., Yasmin, R., Asif, R., Ambreen, A., Mustafa, M. and Umbreen, S., 2022. Green synthesis of silver nanoparticles (AgNPs), structural characterization, and their antibacterial potential. *Dose-Response: A Publication of International Hormesis Society*, 20(1), p.15593258221088709.

Cao, V., Cao, P.A., Han, D.L., Ngo, M.T., Vuong, T.X. and Manh, H.N., 2024. The suitability of Fe3O4/graphene oxide nanocomposite for adsorptive removal of methylene blue and congo red. *Nature Environment & Pollution Technology*, 23(1).

Chan, S.C. and Barteau, M.A., 2005. Preparation of highly uniform Ag/TiO2 and Au/TiO2 supported nanoparticle catalysts by photodeposition. *Langmuir*, 21(12), pp.5588–5595.

Chiu, Y.-H., Chang, T.-F.M., Chen, C.-Y., Sone, M. and Hsu, Y.-J., 2019. Mechanistic insights into photodegradation of organic dyes using heterostructure photocatalysts. *Catalysts*, 9(5), p.430.

Daneshvar, N., Ayazloo, M., Khataee, A.R. and Pourhassan, M., 2007. Biological decolorization of dye solution containing malachite green by microalgae *Cosmarium* sp. *Bioresource Technology*, 98(6), pp.1176-1182.

De Leersnyder, I., De Gelder, L., Van Driessche, I. and Vermeir, P., 2019. Revealing the importance of aging, environment, size and stabilization mechanisms on the stability of metal nanoparticles: a case study for silver nanoparticles in a minimally defined and complex undefined bacterial growth medium. *Nanomaterials (Basel)*, 9(12), p.1684.

Dhankhar, M., Singh, O. and Singh, V.N., 2014. Physical principles of losses in thin film solar cells and efficiency enhancement methods. *Renewable and Sustainable Energy Reviews*, 40, pp.214-223.

Gläsel, J., Diao, J., Feng, Z., Hilgart, M., Wolker, T., Su, D.S. and Etzold, B.J.M., 2015. Mesoporous and graphitic carbide-derived carbons as selective and stable catalysts for the dehydrogenation reaction. *Chemistry of Materials*, 27(16), pp.5719-5725.

Isa, N. and Lockman, Z., 2019. Methylene blue dye removal on silver nanoparticles reduced by *Kyllinga brevifolia*. *Environmental Science and Pollution Research*, 26(11).

Jyoti, K. and Singh, A., 2016. Green synthesis of nanostructured silver particles and their catalytic application in dye degradation. *Journal of Genetic Engineering and Biotechnology*, 14(2), pp.311-317.

Kumar, B.R. and Hymavathi, B., 2017. X-ray peak profile analysis of solid-state sintered alumina doped zinc oxide ceramics by Williamson–Hall and size-strain plot methods. *Journal of Asian Ceramic Societies*, 5(2).

Kumar, R., Rashid, J. and Barakat, M.A., 2015. Zero valent Ag deposited TiO2 for the efficient photocatalysis of methylene blue under UV-C light irradiation. *Colloids and Interface Science Communications*, 5, pp.1-4.

Landi, S., Segundo, I.R., Freitas, E., Vasilevskiy, M., Carneiro, J. and Tavares, C.J., 2022. Use and misuse of the Kubelka-Munk function to obtain the band gap energy from diffuse reflectance measurements. *Solid State Communications*, 341. https://doi.org/10.1016/j.ssc.2021.114573.

Lenzi, G.G., Fávero, C.V.B., Colpini, L.M.S., Bernabe, H., Baesso, M.L., Specchia, S. and Santos, O.A.A., 2011. Photocatalytic reduction of Hg(II) on TiO2 and Ag/TiO2 prepared by the sol-gel and impregnation methods. *Desalination*, 270(1-3), pp.241-247.

Ma, L., Chen, N., Feng, C. and Yang, Q., 2024. Recent advances in enhanced technology of Cr(VI) bioreduction in aqueous condition: A review. *Chemosphere*, 351(3), p.141176.

Melkamu, W.W. and Bitew, L.T., 2021. Green synthesis of silver nanoparticles using *Hagenia abyssinica* (Bruce) J.F. Gmel plant leaf extract and their antibacterial and anti-oxidant activities. *Heliyon*, 7(11).

Mubarak, D.A., Sasikala, M., Gunasekaran, M. and Thajuddin, N., 2011. Biosynthesis and characterization of silver nanoparticles using marine cyanobacterium, *Oscillatoria willei* NTDM01. *Digest Journal of Nanomaterials and Biostructures*, 6(2), pp.385–390.

Nisa, S.K., 2024. Sintesis AgNPs/SAC menggunakan ekstrak empulur pisang (Musa balbisiana) dan aplikasinya sebagai fotokatalis degradasi metilen biru. Skripsi. Universitas Negeri Yogyakarta.

Ong, S.T., Keng, P.S., Nam, L., Tiong, H. and Hung, Y.T., 2011. Dye Waste Treatment. *Water*, 3, pp.157-176.

Prodjosantoso, A.K., Kamilia, S., Utomo, M.P. and Budiasih, K.S., 2019. Silica supported copper-nickel oxide catalyst for photodegradation of methylene blue. *Asian Journal of Chemistry*, 31(12), pp.2891–2896.

Prodjosantoso, A.K., Prawoko, O.S., Utomo, M.P. and Sari, L.P., 2019. Green synthesis of silver nanoparticles using *Salacca zalacca* extract as reducing agent and it’s antibacterial activity. *Asian Journal of Chemistry*, 31(12).

Radha, K.V. and Thamilselvi, V., 2013. Synthesis of silver nanoparticles from *Pseudomonas putida* NCIM 2650 in silver nitrate supplemented growth medium and optimization using response surface methodology. *Digest Journal of Nanomaterials and Biostructures*, 8(3), pp.1101–1111.

Rampe, M.J. and Tiwow, V.A., 2018. Fabrication and characterization of activated carbon from charcoal coconut shell Minahasa, Indonesia. *In Journal of Physics: Conference Series* (Vol. 1028, No. 1, p. 012033). IOP Publishing.

Rizki, I.N., Inoue, T., Chuaicham, C., Shenoy, S., Srikhaow, A., Sekar, K. and Sasaki, K., 2023. Fabrication of reduced Ag nanoparticle using crude extract of cinnamon decorated on ZnO as a photocatalyst for hexavalent chromium reduction. *Catalysts*, 13(2).

Silambarasan, S. and Jayanthi, A., 2013. Biosynthesis of silver nanoparticles using *Pseudomonas fluorescens*. *Research Journal of Biotechnology*, 8(3), pp.71-74.

Sudhakar, P. and Soni, H., 2018. Catalytic reduction of nitrophenols using silver nanoparticles-supported activated carbon derived from agro-waste. *Journal of Environmental Chemical Engineering*, 6(1).

Sun, J., 2014. Development of inorganic-organic hybrid materials for waste water treatment. Thesis. National University of Singapore.

Thenarasu, A., Chai, M.K., Tan, Y.H., Wong, L.S., Rajamani, R. and Djearamane, S., 2024. Study of *Chlorella vulgaris* from different growth phases as biosensor for detection of titanium and silver nanoparticles in water. *Nature Environment & Pollution Technology*, 23(2).

Trinh, V.T., Nguyen, T.M.P., Van, H.T., Hoang, L.P., Nguyen, T.V., Ha, L.T., Vu, X.H., Pham, T.T., Nguyen, T.N., Quang, N.V. and Nguyen, X.C., 2020. Phosphate adsorption by silver nanoparticles-loaded activated carbon derived from tea residue. *Scientific Reports*, 10(1), pp.1-13.

Tuan, T.Q., Son, N., Dung, H.T.K., Luong, N.H., Thuy, B.T., Anh, N.T., Hoa, N.D. and Hai, N.H., 2011. Preparation and properties of silver nanoparticles loaded in activated carbon for biological and environmental applications. *Journal of Hazardous Materials*, 192(3).

Wahyuni, E.T., Roto, R. and Prameswari, M., 2017. TiO2/Ag-nanoparticle as a photocatalyst for dyes degradation. In: *International Conference on Environmental Science and Technology*. CEST.

Wat, M.J., Veenma, D., Hogue, J., Holder, A.M., Yu, Z., Wat, J.J., Hanchard, N., Shchelochkov, O.A., Fernandes, C.J., Johnson, A., Lally, K.P., Slavotinek, A., Danhaive, O., Schaible, T., Cheung, S.W., Rauen, K.A., Tonk, V.S., Tibboel, D., de Klein, A. and Scott, D.A., 2011. Genomic alterations that contribute to the development of isolated and non-isolated congenital diaphragmatic hernia. *Journal of Medical Genetics*, 48(5), pp.299-307.